NIH Public Access
Author Manuscript
*Drug Metab Dispos*. Author manuscript; available in PMC 2009 December 1.

Published in final edited form as:
*Drug Metab Dispos*. 2008 December ; 36(12): 2506–2512. doi:10.1124/dmd.108.022723.

# A double transgenic mouse model expressing human pregnane X receptor and cytochrome P450 3A4

**Xiaochao Ma**, **Connie Cheung**, **Kristopher W. Krausz**, **Yatrik M. Shah**, **Ting Wang**, **Jeffrey R. Idle**, and **Frank J. Gonzalez**
*Laboratory of Metabolism, Center for Cancer Research, National Cancer Institute, National Institutes of Health, Bethesda, MD 20892 (X.M., C.C., K.W.K., Y.S., T.W., and F.J.G.). Institute of Pharmacology, 1st Faculty of Medicine, Charles University, 128 00 Praha 2, Czech Republic (J.R.I.)*

## Abstract

Cytochrome P450 3A4 (CYP3A4), the most abundant human P450 in liver, participates in the metabolism of ~50% of clinically used drugs. The pregnane X receptor (PXR), a member of the nuclear receptor superfamily, is the major activator of CYP3A4 transcription. However, due to species differences in response to PXR ligands, it is problematic to use rodents to assess CYP3A4 regulation and function. The generation of double transgenic mice expressing human PXR and CYP3A4 (TgCYP3A4/hPXR) would provide a means to this problem. In the current study, a TgCYP3A4/hPXR mouse model was generated by bacterial artificial chromosome transgenesis in *Pxr*-null mice. In TgCYP3A4/hPXR mice, CYP3A4 was strongly induced by rifampicin, a human-specific PXR ligand, but not by pregnenolone 16α-carbonitrile, a rodent-specific PXR ligand. Consistent with CYP3A expression, hepatic CYP3A activity increased ~five-fold in TgCYP3A4/hPXR mice pretreated with rifampicin. Most anti-human immunodeficiency virus protease inhibitors are CYP3A substrates and their interactions with rifamycins are a source of major concern in patients co-infected with human immunodeficiency virus and *Mycobacterium tuberculosis*. By using TgCYP3A4/hPXR mice, human PXR-CYP3A4 mediated rifampicin-protease inhibitor interactions were recapitulated, as the metabolic stability of amprenavir, nelfinavir, and saquinavir decreased 52%, 53%, and 99% respectively in the liver microsomes of TgCYP3A4/hPXR mice pretreated with rifampicin. *In vivo*, rifampicin pretreatment resulted in ~80% decrease in the area under serum amprenavir concentration-time curve in TgCYP3A4/hPXR mice. These results suggest that the TgCYP3A4/hPXR mouse model could serve as a useful tool for studies on CYP3A4 transcription and function *in vivo*.

## Introduction

The human cytochrome P450 3A (CYP3A) family is located on chromosome 7q22.1, and consists of four members, 3A4, 3A5, 3A7, and 3A43 (Gellner et al., 2001). Of these, CYP3A4 is the most abundant P450 in liver and small intestine, and participates in the metabolism of approximately 50% of all prescribed drugs, and some endogenous substrates, such as steroids and bile acids (Guengerich, 1999). CYP3A5 expression in humans is highly variable and only ~20% of livers express CYP3A5 (Xie et al., 2004). CYP3A7 is predominantly expressed in fetal liver with a specific role in hydroxylation of retinoic acid and 16α-hydroxylation of steroids (Kitada et al., 1987; Chen et al., 2000). CYP3A43, the most recently discovered

**Corresponding author**: Frank J. Gonzalez, Laboratory of Metabolism, Center for Cancer Research, National Cancer Institute, Building 37, Room 3106, Bethesda, MD 20892. Tel: 301 496 9067. Fax: 301 496 8419. Email: E-mail: fjgonz@helix.nih.gov.
The current address of XM is Department of Pharmacology, Toxicology and Therapeutics, University of Kansas Medical Center, Kansas City, KS 66160. The current address of CC is Department of Chemical Biology,□Laboratory for Cancer Research,□College of Pharmacy, Rutgers University,□Piscataway, N.J. 08854.

NIH-PA Author Manuscript
NIH-PA Author Manuscript
NIH-PA Author Manuscript

NIH-PA Author Manuscript

NIH-PA Author Manuscript

NIH-PA Author Manuscript

CYP3A, is expressed in prostate and testis with low level expression in liver (Westlind et al., 2001). Among the CYP3A members, CYP3A4 is the most critical P450 for drug metabolism. Due to its broad substrate spectrum, CYP3A4 contributes to many adverse drug-drug interactions (Guengerich, 1999).

Pregnane X receptor (PXR) is the dominant activator controlling *CYP3A4* transcription (Lehmann et al., 1998; Xie et al., 2000). Following ligand binding, human PXR forms a heterodimer with the retinoid X receptor, and subsequently binds to PXR response elements in the 5′-flanking region of the *CYP3A4* gene resulting in increased transcription (Goodwin et al., 2003). PXR is activated by a large number of prescription drugs, herbal supplements, vitamins, and some endobiotics (Carnahan and Redinbo, 2005). Interestingly, there are significant species differences in response to PXR ligands between humans and rodents (Jones et al., 2000). Drugs such as rifampicin (RIF), clotrimazole, and troglitazone activate human PXR but are weak activators of rodent PXR. In contrast, dexamethasone and pregnenolone 16α-carbonitrile (PCN) activate rodent PXR but are weak activators of human PXR. Therefore the *CYP3A4*-transgenic mouse models that have been generated are of limited utility for transcriptional and drug interaction studies because of their mouse PXR background (Granvil et al., 2003; Robertson et al., 2003; Zhang et al., 2003; Zhang et al., 2004; Cheung et al., 2006). The generation of double transgenic mice expressing human PXR and CYP3A4 would provide a solution to this problem.

In the current study, a double transgenic mouse model was generated by bacterial artificial chromosome (BAC) transgenesis with human PXR and CYP3A4 in *Pxr*-null mice, and designated TgCYP3A4/hPXR mice. Treatment of TgCYP3A4/hPXR mice with the PXR ligands mimicked the human response, since CYP3A4 was strongly induced by RIF, a human-specific PXR ligand, but not by PCN, a rodent-specific PXR ligand. Most antihuman immunodeficiency virus (HIV) protease inhibitors (PI) are CYP3A substrates, and their interactions with rifamycins is a major issue in patients co-infected with *Mycobacterium tuberculosis* (TB) and HIV (Breen et al., 2006; Swaminathan et al., 2006; Ribera et al., 2007). By using TgCYP3A4/hPXR mice, human PXR-CYP3A4 mediated RIF-PIs interactions were illustrated, thus demonstrating the utility of this mouse model for studies on CYP3A4 transcription and function.

## Materials and methods

### Chemicals

Rifampicin (RIF), pregnenolone 16α-carbonitrile (PCN), midazolam (MDZ), ketoconazole, and NADPH were obtained from Sigma-Aldrich (St. Louis MO). 1′-Hydroxymidazolam (1′-OH-MDZ) was purchased from BD Gentest (Woburn, MA). Amprenavir (APV), nelfinavir (NFV), and saquinavir (SQV) were supplied by the NIH AIDS Research and Reference Reagent Program. All other chemicals were of the highest grade commercially available.

### Generation of double transgenic mice expressing human PXR and CYP3A4 (TgCYP3A4/hPXR)

The TgCYP3A4/hPXR mouse line was generated by bacterial artificial chromosome (BAC) transgenesis. The BAC clone RP11-757A13 (123,778 bp) contains the complete *CYP3A4* and *CYP3A7* genes including 5′- and 3′-flanking sequences (Fig 1A), and the BAC clone RP11-169N13 (165,093 bp) contains the complete human *PXR* gene sequence including 5′- and 3′-flanking sequences (Fig 1B). Both BAC clones were obtained from Resgen/Invitrogen Corporation (Huntsville, AL), and purified using a maxi prep kit (Qiagen, Valencia, CA). The BAC clone for *CYP3A4* was verified by southern blot analysis with $^{32}$P-end-labeled CYP3A4 cDNA and DNA oligonucleotide probes recognizing specific regions (exons 1 and 13, -10 kb

NIH-PA Author Manuscript

NIH-PA Author Manuscript

NIH-PA Author Manuscript

upstream) of the human *CYP3A4* gene (Cheung et al., 2006). The BAC clone for human PXR was verified by PCR using primers designed to amplify specific regions within exons 2 and 9, and the 5′ UTR (Ma et al., 2007). Two major steps were carried out to generate the TgCYP3A4/hPXR mice. Step I: the *CYP3A4*-transgenic mice (TgCYP3A4) was bred with *Pxr*-null mice to generate the TgCYP3A4/*Pxr*-null mouse line; Step II: the *PXR*-humanized mice (hPXR) were bred with the TgCYP3A4/*Pxr*-null mice to generate the TgCYP3A4 mouse containing human PXR. Mice positive for the human *PXR* and *CYP3A4* transgenes and containing the mouse *Pxr*-null allele, as determined by PCR genotyping, were designated TgCYP3A4/hPXR mice. *Pxr*-null, TgCYP3A4 and hPXR mice were described previously (Staudinger et al., 2001;Cheung et al., 2006;Ma et al., 2007).

## PCR genotyping

The presence of the *CYP3A4* transgene was determined using the following primers, Fwd 5′-TGG AAT GAG GAC AGC CAT AGA GAC -3′ and Rev 5′- AGA AGA GGA GCC TGG ACA GTT ACT C -3′, amplifying a PCR product of 521 bp in the samples only positive for human *CYP3A4* transgene (Cheung et al., 2006). Mouse epoxide hydrolase 1 gene primers served as an internal positive control for amplification, yielding a fragment of 341 bp in all samples (Miyata et al., 1999). The presence of the human *PXR* transgene was determined using the following primers, Fwd 5′- GCA CCT GCT GCT AGG GAA TA-3′ and Rev 5′-CTC CAT TGC CCC TCC TAA GT-3′, amplifying a PCR product of 576 bp in the samples only positive for human *PXR* transgene (Ma et al., 2007). The following primers were used to identify the mouse *Pxr* wild-type and null alleles, Fwd 5′- CTG GTC ATC ACT GTT GCT GTA CCA-3′, Rev1 5′- GCA GCA TAG GAC AAG TTA TTC TAG AG-3′ and Rev2 5′- CTA AAG CGC ATG CTC CAG ACT GC-3′, amplifying a PCR product of 348 bp for wild-type allele and 265 bp for *Pxr*-null allele (Guo et al., 2003).

## Animals and treatments

TgCYP3A4/hPXR, TgCYP3A4 and wild-type mice (WT) were maintained under a standard 12 h light/12 h dark cycle with water and chow provided *ad libitum*. Handling was in accordance with animal study protocols approved by the National Cancer Institute Animal Care and Use Committee. Since it was previously shown in TgCYP3A4 mice that age and gender were determinants of hepatic CYP3A4 expression (Cheung et al., 2006), both male and female TgCYP3A4/hPXR mice were used and liver samples collected from 2-, 4-, 6-, 8-, 16-, and 24-week-old mice. For analysis of CYP3A4 tissue distribution, liver, lung, small intestine, kidney, heart, ovary or testis were collected at 4 weeks of age. For studies on hepatic CYP3A4 regulation by xenobiotics, TgCYP3A4/hPXR and TgCYP3A4 mice (8-10 weeks old) were treated with 10 mg/kg PCN (ip), or with 10 mg/kg RIF (po), once daily for 3 days. All mice were killed by $CO_2$ asphyxiation, and samples were collected and frozen at -80°C for further analysis.

## Microsome preparation and western blot analysis

All tissues were homogenized in ice-cold buffer (50 mM Tris-HCl, 150 mM KCl, 1 mM EDTA and 20% glycerol). Microsomes were prepared by centrifugation at 10,000 *g* for 20 min at 4° C, and the resulting supernatant spun at 100,000 *g* for 1 hr at 4°C. Microsomal pellets were resuspended in the same ice-cold buffer used for homogenization. Protein concentrations were determined using a BCA Protein Assay Kit (Pierce Chemical Co., Rockford, IL). For western blot analysis, microsomal protein (10 μg) from each sample was loaded onto 10% polyacrylamide SDS-PAGE gels and electrophoretically transferred to nitrocellulose membranes (Schleicher & Schuell, Keene, NH). Immunoblot analysis was carried out using antibodies to human CYP3A4 (mAb 275-1-2), rat CYP3A1 (mAb 2-13-1) (Gelboin et al., 1995), and GAPDH (Chemicon International, Temecula, CA). Corresponding secondary

NIH-PA Author Manuscript

NIH-PA Author Manuscript

NIH-PA Author Manuscript

antibodies were purchased from Jackson ImmunoResearch Laboratories, Inc (West Grove, PA). Immunoreactive proteins were detected with an ECL kit (Pierce Chemical Co., Rockford, IL) following the manufacturer's instructions.

### CYP3A activity analysis

Hepatic CYP3A activity was detected by using liver microsomes. MDZ 1′-hydroxylation was used as a probe for CYP3A activity, and the method for CYP3A activity analysis was described previously (Thummel et al., 1994; Ma et al., 2007). Briefly, incubations were carried out in 100 mM sodium phosphate buffer (pH 7.4) containing microsomes with 100 μg of protein, and 50 μM MDZ. Ketoconazole (5 μM) was used as CYP3A inhibitor and pre-incubated at 37°C for 5 min. The reaction was initiated by the addition of 20 μl of 20 mM NADPH, 37°C for 10 min, and terminated by the addition of 1 ml ethyl acetate and 1 ml methyl *t*-butyl ether mixture. Samples were centrifuged at 3,000 rpm for 5 min at 4°C. The organic layer was then transferred to a new tube, dried with $N_2$ and reconstituted in 100 μl of 70% methanol and 30% $H_2O$ containing 0.1% formic acid. Six μl of the reconstituted solution was injected to liquid chromatography-coupled tandem mass spectrometry (LC-MS/MS) for 1′-OH-MDZ detection. All reactions were performed in duplicate.

### Metabolic stability of HIV protease inhibitors (PIs)

The PIs metabolic stability was analyzed by using liver microsomes of TgCYP3A4/hPXR and WT mice pretreated with or without RIF. The incubations were performed in 100 mM sodium phosphate buffer (pH 7.4) containing microsomes with 100 μg of protein, and 10 μM PIs (APV, NFV, or SQV) in a final volume of 200 μl. The reactions were initiated by the addition of 20 μl of 20 mM NADPH, 37°C for 10 min, and terminated by the addition of 200 μl methanol. The mixtures were vortexed and centrifuged at 12,000 rpm for 10 min at 4°C. Six μl of the de-proteinized mixtures were injected to an LC-MS/MS for detection of the parent drugs. By monitoring parent drug disappearance, the metabolic stability of PIs was determined according to their metabolic rates. Metabolic stability of MDZ was used as positive control for these experiments.

### Pharmacokinetic study of amprenavir in TgCYP3A4/hPXR mice

TgCYP3A4/hPXR mice were treated with AIN-93G purified rodent diet (control) or modified AIN-93G rodent diet with 100 mg/kg RIF (Dyets Inc., Bethlehem, PA) for 6 days. On the $7^{th}$ day, TgCYP3A4/hPXR mice were administered 50 mg/kg APV orally by gavage. Blood samples were collected from suborbital veins using heparinized tubes at 0, 0.25, 0.5, 1, 2, 4, 8, 18 hours after administration of APV. Serum was separated by centrifugation at 8000g for 10 min. For APV analysis, 15 μl of serum was mixed with 85 μl of $H_2O$, 100 μl of methanol. The mixture was vortexed and centrifuged at 12,000 rpm for 10 min at 4°C. Six μl of the de-proteinized mixture was injected to an LC-MS/MS for detection of the parent drugs. Pharmacokinetic parameters for APV were estimated from the plasma concentration-time data by a noncompartmental approach using WinNonlin (Pharsight, Mountain View, CA). The maximum concentration in serum (*C*max) was obtained from the original data. The area under the serum concentration-time curve ($AUC_{0\text{-}18\ hour}$) was calculated by the trapezoidal rule.

### LC-MS/MS analysis

MDZ, MDZ metabolites and PIs were analyzed using previously described LC-MS/MS methods with slight modification (Granvil et al., 2003; Crommentuyn KM et al., 2003). Briefly, LC-MS/MS analysis was carried out using a high-performance liquid chromatography system consisting of a PerkinElmer Series 200 quaternary pump, vacuum degasser, Luna C18 50 mm × 4.6 mm *i.d.* column (Phenomenex, Torrance, CA), and auto-sampler with a 100 μl loop interfaced to an API2000 SCIEX triple-quadrupole tandem mass spectrometer (Applied

NIH-PA Author Manuscript

NIH-PA Author Manuscript

NIH-PA Author Manuscript

Biosystems/MDS Sciex, Foster City, CA). The flow rate through the column at ambient temperature was 0.25 ml/min with 70% methanol and 30% $H_2O$ containing 0.1% formic acid. Each analysis lasted for 5.0 min. The mass spectrometer was operated in the turbo ion spray mode with positive ion detection. The turbo ion spray temperature was maintained at 300°C, and a voltage of 4.8 kV was applied to the sprayer needle. $N_2$ was used as the turbo ion spray and nebulizing gas. The detection and quantification of analysts were performed using the multiple reactions monitoring mode, with m/z 326/291 for MDZ, m/z 342/203 for 1′-OH-MDZ, m/z 506/245 for APV, m/z 568/330 for NFV, and m/z 671/570 for SQV. For these chemicals, the detection limits were 0.1-0.2 pmol. The curve range was 0.039 to 10 μM with the linearity's above 98%.

### Statistical analysis

All values are expressed as the means ± SD and group differences are analyzed by Student's *t* test.

## Results

### Generation of TgCYP3A4/hPXR mice

TgCYP3A4/hPXR mice were generated by BAC transgenesis with the complete *CYP3A4*, *CYP3A7* and human *PXR* gene sequences in a mouse *Pxr* null background (Fig 1A and 1B). Typical PCR genotyping results are shown in Fig 1C. TgCYP3A4 mice were positive for the human *CYP3A4* transgene and containing the mouse *Pxr* allele. The TgCYP3A4/hPXR mice were positive for both the human *PXR* and *CYP3A4* transgenes and containing the mouse *Pxr* null allele.

### CYP3A4 expression in TgCYP3A4/hPXR mice

CYP3A4 protein was analyzed by western blot. Four-week-old TgCYP3A4/hPXR male and female mice demonstrated expression of CYP3A4 in liver and small intestine but not in the lung, kidney, heart, or testis/ovary (Fig 2A and 2B), which is consistent with the tissue distribution of Cyp3a in mice and CYP3A4 in humans (Guengerich, 1999). Interestingly, the developmental expression patterns for hepatic CYP3A4 protein showed significant gender difference between the ages of 2 to 24 weeks. In TgCYP3A4/hPXR male mice, hepatic CYP3A4 was detected in 2-and 4-week-old, but not in mice over 6-weeks-old mice (Fig 2C), which suggests transcriptional down-regulation of basal CYP3A4 expression following sexual maturity in males. However, female mice expressed hepatic CYP3A4 at all time points assessed from 2 to 24 weeks of age (Fig 2D). In contrast to the absent expression of hepatic CYP3A4 in adult males, the human PXR was constantly expressed in the liver of TgCYP3A4/hPXR mice (data not shown).

### Regulation of hepatic CYP3A4 expression in TgCYP3A4/hPXR mice

The regulation of CYP3A4 expression in TgCYP3A4/hPXR mice was compared with TgCYP3A4 mice. The BAC clone used for establishing the TgCYP3A4/hPXR and TgCYP3A4 mice was the same in both lines. In TgCYP3A4 mice, endogenous mouse *PXR* is present whereas the TgCYP3A4/hPXR mice contain the human *PXR* with a mouse *Pxr*-null allele. TgCYP3A4/hPXR and TgCYP3A4 mice were treated with the human PXR ligand RIF and rodent PXR ligand PCN. Hepatic CYP3A4 was detected by western blot analysis. In adult male mice, CYP3A4 was not detected in the control TgCYP3A4/hPXR and TgCYP3A4 mice. After PCN treatment, CYP3A4 was induced strongly in TgCYP3A4 mice, but only slightly in TgCYP3A4/hPXR mice. RIF treatment did not increase CYP3A4 in TgCYP3A4 mice while induction of CYP3A4 was robust in TgCYP3A4/hPXR mice (Fig 3A). The regulation of CYP3A4 expression in female TgCYP3A4/hPXR mice was similar to male mice (Fig 3B).

NIH-PA Author Manuscript

NIH-PA Author Manuscript

NIH-PA Author Manuscript

The human PXR in TgCYP3A4/hPXR mice was also functional in regulation of mouse PXR target genes. Following RIF treatment, mouse hepatic Cyp3a11, glutathione S-transferase A1, and organic anion transporting polypeptide 2 were all induced significantly in TgCYP3A4/hPXR mice (data not shown).

### Hepatic CYP3A activity in TgCYP3A4/hPXR mice

In TgCYP3A4/hPXR mice pretreated with RIF, both hepatic human CYP3A4 and mouse Cyp3a were induced. Consistent with CYP3A expression, hepatic CYP3A activity increased significantly in TgCYP3A4/hPXR mice after PXR ligand treatment. In WT and TgCYP3A4 mice, RIF produced no significant effect on CYP3A activity (Fig 4A and 4B). However, in TgCYP3A4/hPXR mice pretreated with RIF, CYP3A activity increased ~five-fold compared with the vehicle-treated control group (Fig 4C), and it was markedly inhibited by the CYP3A inhibitor ketaconazole (Fig 4D).

### PXR-CYP3A mediated drug-drug interactions in TgCYP3A4/hPXR mice

Most clinically used HIV PIs are CYP3A substrates, such as APV, SQV, and NFV, and their interactions with rifamycins are of concern in patients co-infected with TB and HIV (Breen et al., 2006; Swaminathan et al., 2006; Ribera et al., 2007). Human PXR-CYP3A4 mediated RIF-PIs interactions were assessed in TgCYP3A4/hPXR mice. PXR activation and CYP3A induction accelerated the metabolism of PIs. In liver microsomes from TgCYP3A4/hPXR mice pretreated with RIF, the metabolic stability of APV, NFV, and SQV decreased 52%, 53%, and 99% respectively, but no significant change was observed in liver microsomes of WT mice (Fig 5). In TgCYP3A4/hPXR mice pretreated with RIF, both human CYP3A4 and mouse Cyp3a in the liver and small intestine were induced; most significantly, hepatic CYP3A4, which was not expressed in the control group, was highly expressed after PXR activation (Fig 6A). Consistent with the *in vitro* study, the pharmacokinetic analysis demonstrated that the *C*max of serum APV concentration decreased by ~93% and the $AUC_{0\text{-}18\ hours}$ of APV decreased by ~80% in TgCYP3A4/hPXR mice pretreated with RIF (Fig 6B). These data revealed a significant effect of RIF on human PXR activation and CYP3A regulation, and indicated that RIF-PIs interactions were mediated by human PXR and CYP3A.

## Discussion

In the current study, a double transgenic mouse model expressing human PXR and CYP3A4 was generated by BAC transgenesis in *Pxr*-null mice. Compared to the previously generated *CYP3A4*-transgenic mouse models (Granvil et al., 2003; Robertson et al., 2003; Zhang et al., 2003; Zhang et al., 2004; Cheung et al., 2006), the major improvement in the current model was the inclusion of human PXR, the dominant activator of CYP3A4 transcription. All previous CYP3A4 mouse models were generated on a mouse PXR background, which does not mimic human CYP3A4 regulation because of the species differences in PXR in response to various ligands. The current mouse model improves upon these earlier mouse lines since the human CYP3A4 transgenic mouse was generated on a human PXR background. Treatment with PXR ligands in TgCYP3A4/hPXR mice mimicked the human response, as demonstrated by the robust induction of CYP3A4 by the human-specific PXR ligand RIF and weak CYP3A4 induction by the rodent specific PXR ligand PCN. Consistent with CYP3A expression, hepatic CYP3A activity significantly increased in TgCYP3A4/hPXR mice treated with RIF. These results revealed that the TgCYP3A4/hPXR mouse model would be a useful tool for the study of CYP3A4 transcription and function.

Because of the importance of CYP3A4 in drug metabolism, multiple *in vitro* and *in vivo* models had been generated for studies on CYP3A4. *CYP3A4*-expressing cell lines were produced using Chinese hamster CHL cells, yeast, and Escherichia coli (Brian et al., 1990; Zhou et al., 2001;

NIH-PA Author Manuscript

NIH-PA Author Manuscript

NIH-PA Author Manuscript

Yamazaki et al., 2002). *CYP3A4*-expressing cell lines were demonstrated to be of value in the functional analysis of CYP3A4 but are limited for the study of CYP3A4 transcription and drug-drug interactions using PXR activators. By using the primary cultures of human hepatocytes, transcriptional regulation and expression of CYP3A4 was recapitulated (Luo et al., 2004; Martinez-Jimenez et al., 2007). However, other CYP3A4 models should be considered due to the limited availability of human hepatocytes, and the limitation of extrapolating *in vitro* findings to the *in vivo* situation. The development of *CYP3A4*-transgenic mouse models provides a means to overcome the limitations of *in vitro* models. *CYP3A4*-transgenic mouse models are valuable tools for studying the function and regulation of CYP3A4 in a whole animal system, and the functional significance of CYP3A4 expression can be evaluated under controlled conditions (Gonzalez and Yu, 2006). Previously, several *CYP3A4*-transgenic mouse models were generated (Granvil et al., 2003; Robertson et al., 2003; Zhang et al., 2003; Zhang et al., 2004; Cheung et al., 2006). However, all of these mouse models are limited in transcriptional studies on CYP3A4 because of their mouse PXR background. The advantage of TgCYP3A4/hPXR mouse model described in the current study is its human PXR background, which mimicked the human response to xenobiotics as PXR activators.

In TgCYP3A4/hPXR mice, the basal expression of CYP3A4 in liver exhibited developmental expression characterized by sexual dimorphism in postpuberty. In female TgCYP3A4/hPXR mice, hepatic CYP3A4 was expressed constantly; however in male mice, there was no hepatic CYP3A4 expression after sexual maturity. This phenomenon was also recorded in the previously generated two TgCYP3A4 mouse lines (Yu et al., 2005; Cheung et al., 2006). In humans, CYP3A4 expression increases during development from childhood to adulthood, but it is not clear whether CYP3A4 expression is sex-dependent, and the conclusion on the gender difference of hepatic CYP3A activity remains uncertain although the trend exists for higher expression in females (Schmucker et al., 1990; Wolbold et al., 2003). Indeed, the sex specificity of CYP3A4 in humans is affected by multiple factors, such as dietary supplements, drinking, smoking, and medication history which could affect expression levels through increased PXR-mediated induction. These factors can be controlled in the case of animals maintained under defined dietary and environmental conditions, suggesting that mouse models may be useful for investigation of the sexual dimorphism and developmental expression of CYP3A4. For example, it was demonstrated that growth hormone regulated the sexual dimorphism in the developmental expression of the CYP3A4 transgene (Cheung et al., 2006). The major difference between the current mouse model and the previous TgCYP3A4 mouse models is the human PXR background; however all TgCYP3A4 male mice showed similar hepatic CYP3A4 expression levels and regulation thus suggesting that human PXR does not affect basal CYP3A4 expression.

The most common clinical implication for human PXR activation is the occurrence of drug-drug interactions mediated by the up-regulated CYP3A4. The adverse interactions of rifamycins and PIs for anti-HIV are typical examples of human PXR-CYP3A mediated drug-drug interactions. According to the World Health Organization, about 13 million people living with HIV worldwide are co-infected with TB, and TB accounts for up to one-third of HIV patients' deaths. PIs are commonly used for anti-HIV treatment, and these drugs are generally metabolized by CYP3A4. Rifamycins are widely used drugs for TB treatment; however they are also human PXR activators. Significant drug-drug interactions were noted in clinical treatment with rifamycins and PIs. Around 60% to 90% plasma levels of PIs decreased when combined with RIF (Niemi et al., 2003), which led to concern with the use of combined therapies for patients co-effected with HIV and TB (Breen et al., 2006; Swaminathan et al., 2006; Ribera et al., 2007). It is difficult to predict and manage drug-drug interactions mediated by human PXR and CYP3A4 in rodents due to the species differences in response to PXR ligands. By using TgCYP3A4/hPXR mice, human PXRCYP3A4 mediated RIF-PIs interactions were revealed. A decrease in the $AUC_{0\text{-}18}$ of APV in TgCYP3A4/hPXR mice

NIH-PA Author Manuscript

NIH-PA Author Manuscript

NIH-PA Author Manuscript

following RIF treatment was observed, similar to what was reported in humans (Polk et al., 2001). These data suggest that the TgCYP3A4/hPXR mouse is a useful tool for *in vivo* studies on the drug-drug interactions between PXR ligands and CYP3A substrates. However, it should be noted that data generated with this mouse model should be interpreted with caution since the hepatic blood flow rates and the distribution of CYP3A between hepatic and enteric sites may not precisely mimic humans, especially with the wide interindividual variation in expression in the human population.

In conclusion, a double transgenic mouse model expressing human PXR and CYP3A4 was generated successfully by BAC transgenesis. This mouse model provides a means for studying the regulation and function of human *CYP3A4* gene in a whole animal model.

## Acknowledgements

We thank the NIH AIDS Research and Reference Reagent Program for the support of HIV protease inhibitors. We thank John R. Buckley for technical assistance.

This study was funded by the NCI Intramural Research Program. JRI is grateful to U.S. Smokeless Tobacco Company for a grant for collaborative research.

## Abbreviations

PXR, pregnane X receptor
CYP, cytochrome P450
BAC, bacterial artificial chromosome
TgCYP3A4, *CYP3A4*-transgenic mice
hPXR, *PXR*-humanized mice
TgCYP3A4/hPXR, double transgenic mice expressing human PXR and CYP3A4
WT, wild-type mice
RIF, rifampicin
PCN, pregnenolone 16α-carbonitrile
MDZ, midazolam
1′-OH-MDZ, 1′-hydroxymidazolam
TB, Mycobacterium tuberculosis
HIV, human immunodeficiency virus
PI, protease inhibitor
APV, amprenavir
NFV, nelfinavir
SQV, saquinavir
LC-MS/MS, liquid chromatographic tandem mass spectrometric
qPCR, quantitative real-time polymerase chain reaction
*C*max, maximum concentration
AUC, area under concentration-time curve

## References

Breen RA, Swaden L, Ballinger J, Lipman MC. Tuberculosis and HIV coinfection: a practical therapeutic approach. Drugs 2006;66:2299–2308. [PubMed: 17181373]

Brian WR, Sari MA, Iwasaki M, Shimada T, Kaminsky LS, Guengerich FP. Catalytic activities of human liver cytochrome P-450 IIIA4 expressed in Saccharomyces cerevisiae. Biochemistry 1990;29:11280–11292. [PubMed: 2271712]

Carnahan VE, Redinbo MR. Structure and function of the human nuclear xenobiotic receptor PXR. Curr Drug Metab 2005;6:357–367. [PubMed: 16101574]

NIH-PA Author Manuscript

NIH-PA Author Manuscript

NIH-PA Author Manuscript

Crommentuyn KM, Rosing H, Nan-Offeringa LG, Hillebrand MJ, Huitema AD, Beijnen JH. Rapid quantification of HIV protease inhibitors in human plasma by high-performance liquid chromatography coupled with electrospray ionization tandem mass spectrometry. J Mass Spectrom 2003;38:157–166. [PubMed: 12577282]

Chen H, Fantel AG, Juchau MR. Catalysis of the 4-hydroxylation of retinoic acids by cyp3a7 in human fetal hepatic tissues. Drug Metab Dispos 2000;28:1051–1057. [PubMed: 10950848]

Cheung C, Yu AM, Chen CS, Krausz KW, Byrd LG, Feigenbaum L, Edwards RJ, Waxman DJ, Gonzalez FJ. Growth hormone determines sexual dimorphism of hepatic cytochrome P450 3A4 expression in transgenic mice. J Pharmacol Exp Ther 2006;316:1328–1334. [PubMed: 16291874]

Gelboin HV, Krausz KW, Goldfarb I, Buters JT, Yang SK, Gonzalez FJ, Korzekwa KR, Shou M. Inhibitory and non-inhibitory monoclonal antibodies to human cytochrome P450 3A3/4. Biochem Pharmacol 1995;50:1841–1850. [PubMed: 8615863]

Gellner K, Eiselt R, Hustert E, Arnold H, Koch I, Haberl M, Deglmann CJ, Burk O, Buntefuss D, Escher S, Bishop C, Koebe HG, Brinkmann U, Klenk HP, Kleine K, Meyer UA, Wojnowski L. Genomic organization of the human CYP3A locus: identification of a new, inducible CYP3A gene. Pharmacogenetics 2001;11:111–121. [PubMed: 11266076]

Gonzalez FJ, Yu AM. Cytochrome P450 and xenobiotic receptor humanized mice. Annu Rev Pharmacol Toxicol 2006;46:41–64. [PubMed: 16402898]

Goodwin B, Gauthier KC, Umetani M, Watson MA, Lochansky MI, Collins JL, Leitersdorf E, Mangelsdorf DJ, Kliewer SA, Repa JJ. Identification of bile acid precursors as endogenous ligands for the nuclear xenobiotic pregnane X receptor. Proc Natl Acad Sci U S A 2003;100:223–228. [PubMed: 12509506]

Granvil CP, Yu AM, Elizondo G, Akiyama TE, Cheung C, Feigenbaum L, Krausz KW, Gonzalez FJ. Expression of the human CYP3A4 gene in the small intestine of transgenic mice: in vitro metabolism and pharmacokinetics of midazolam. Drug Metab Dispos 2003;31:548–558. [PubMed: 12695342]

Guengerich FP. Cytochrome P-450 3A4: regulation and role in drug metabolism. Annu Rev Pharmacol Toxicol 1999;39:1–17. [PubMed: 10331074]

Guo GL, Lambert G, Negishi M, Ward JM, Brewer HB Jr. Kliewer SA, Gonzalez FJ, Sinal CJ. Complementary roles of farnesoid X receptor, pregnane X receptor, and constitutive androstane receptor in protection against bile acid toxicity. J Biol Chem 2003;278:45062–45071. [PubMed: 12923173]

Jones SA, Moore LB, Shenk JL, Wisely GB, Hamilton GA, McKee DD, Tomkinson NC, LeCluyse EL, Lambert MH, Willson TM, Kliewer SA, Moore JT. The pregnane X receptor: a promiscuous xenobiotic receptor that has diverged during evolution. Mol Endocrinol 2000;14:27–39. [PubMed: 10628745]

Kitada M, Kamataki T, Itahashi K, Rikihisa T, Kanakubo Y. P-450 HFLa, a form of cytochrome P-450 purified from human fetal livers, is the 16 alpha-hydroxylase of dehydroepiandrosterone 3-sulfate. J Biol Chem 1987;262:13534–13537. [PubMed: 3654629]

Lehmann JM, McKee DD, Watson MA, Willson TM, Moore JT, Kliewer SA. The human orphan nuclear receptor PXR is activated by compounds that regulate CYP3A4 gene expression and cause drug interactions. J Clin Invest 1998;102:1016–1023. [PubMed: 9727070]

Luo G, Guenthner T, Gan LS, Humphreys WG. CYP3A4 induction by xenobiotics: biochemistry, experimental methods and impact on drug discovery and development. Curr Drug Metab 2004;5:483–505. [PubMed: 15578943]

Ma X, Shah Y, Cheung C, Guo GL, Feigenbaum L, Krausz KW, Idle JR, Gonzalez FJ. The PREgnane X receptor gene-humanized mouse: a model for investigating drug-drug interactions mediated by cytochromes P450 3A. Drug Metab Dispos 2007;35:194–200. [PubMed: 17093002]

Martinez-Jimenez CP, Jover R, Donato MT, Castell JV, Gomez-Lechon MJ. Transcriptional regulation and expression of CYP3A4 in hepatocytes. Curr Drug Metab 2007;8:185–194. [PubMed: 17305497]

Miyata M, Kudo G, Lee YH, Yang TJ, Gelboin HV, Fernandez-Salguero P, Kimura S, Gonzalez FJ. Targeted disruption of the microsomal epoxide hydrolase gene. Microsomal epoxide hydrolase is required for the carcinogenic activity of 7,12-dimethylbenz[a]anthracene. J Biol Chem 1999;274:23963–23968. [PubMed: 10446164]

NIH-PA Author Manuscript

NIH-PA Author Manuscript

NIH-PA Author Manuscript

Niemi M, Backman JT, Fromm MF, Neuvonen PJ, Kivisto KT. Pharmacokinetic interactions with rifampicin : clinical relevance. Clin Pharmacokinet 2003;42:819–850. [PubMed: 12882588]

Polk RE, Brophy DF, Israel DS, Patron R, Sadler BM, Chittick GE, Symonds WT, Lou Y, Kristoff D, Stein DS. Pharmacokinetic Interaction between amprenavir and rifabutin or rifampin in healthy males. Antimicrob Agents Chemother 2001;45:502–508. [PubMed: 11158747]

Ribera E, Azuaje C, Lopez RM, Domingo P, Curran A, Feijoo M, Pou L, Sanchez P, Sambeat MA, Colomer J, Lopez-Colomes JL, Crespo M, Falco V, Ocana I, Pahissa A. Pharmacokinetic interaction between rifampicin and the once-daily combination of saquinavir and low-dose ritonavir in HIV-infected patients with tuberculosis. J Antimicrob Chemother 2007;59:690–697. [PubMed: 17307771]

Robertson GR, Field J, Goodwin B, Bierach S, Tran M, Lehnert A, Liddle C. Transgenic mouse models of human CYP3A4 gene regulation. Mol Pharmacol 2003;64:42–50. [PubMed: 12815159]

Schmucker DL, Woodhouse KW, Wang RK, Wynne H, James OF, McManus M, Kremers P. Effects of age and gender on in vitro properties of human liver microsomal monooxygenases. Clin Pharmacol Ther 1990;48:365–374. [PubMed: 2121408]

Staudinger JL, Goodwin B, Jones SA, Hawkins-Brown D, MacKenzie KI, LaTour A, Liu Y, Klaassen CD, Brown KK, Reinhard J, Willson TM, Koller BH, Kliewer SA. The nuclear receptor PXR is a lithocholic acid sensor that protects against liver toxicity. Proc Natl Acad Sci U S A 2001;98:3369–3374. [PubMed: 11248085]

Swaminathan S, Luetkemeyer A, Srikantiah P, Lin R, Charlebois E, Havlir DV. Antiretroviral therapy and TB. Trop Doct 2006;36:73–79. [PubMed: 16611437]

Thummel KE, Shen DD, Podoll TD, Kunze KL, Trager WF, Hartwell PS, Raisys VA, Marsh CL, McVicar JP, Barr DM, et al. Use of midazolam as a human cytochrome P450 3A probe: I. In vitro-in vivo correlations in liver transplant patients. J Pharmacol Exp Ther 1994;271:549–556. [PubMed: 7965755]

Westlind A, Malmebo S, Johansson I, Otter C, Andersson TB, Ingelman-Sundberg M, Oscarson M. Cloning and tissue distribution of a novel human cytochrome p450 of the CYP3A subfamily, CYP3A43. Biochem Biophys Res Commun 2001;281:1349–1355. [PubMed: 11243885]

Wolbold R, Klein K, Burk O, Nussler AK, Neuhaus P, Eichelbaum M, Schwab M, Zanger UM. Sex is a major determinant of CYP3A4 expression in human liver. Hepatology 2003;38:978–988. [PubMed: 14512885]

Xie HG, Wood AJ, Kim RB, Stein CM, Wilkinson GR. Genetic variability in CYP3A5 and its possible consequences. Pharmacogenomics 2004;5:243–272. [PubMed: 15102541]

Xie W, Barwick JL, Downes M, Blumberg B, Simon CM, Nelson MC, Neuschwander-Tetri BA, Brunt EM, Guzelian PS, Evans RM. Humanized xenobiotic response in mice expressing nuclear receptor SXR. Nature 2000;406:435–439. [PubMed: 10935643]

Yamazaki H, Nakamura M, Komatsu T, Ohyama K, Hatanaka N, Asahi S, Shimada N, Guengerich FP, Shimada T, Nakajima M, Yokoi T. Roles of NADPHP450 reductase and apo- and holo-cytochrome b5 on xenobiotic oxidations catalyzed by 12 recombinant human cytochrome P450s expressed in membranes of Escherichia coli. Protein Expr Purif 2002;24:329–337. [PubMed: 11922748]

Yu AM, Fukamachi K, Krausz KW, Cheung C, Gonzalez FJ. Potential role for human cytochrome P450 3A4 in estradiol homeostasis. Endocrinology 2005;146:2911–2919. [PubMed: 15817670]

Zhang W, Purchio AF, Chen K, Wu J, Lu L, Coffee R, Contag PR, West DB. A transgenic mouse model with a luciferase reporter for studying in vivo transcriptional regulation of the human CYP3A4 gene. Drug Metab Dispos 2003;31:1054–1064. [PubMed: 12867495]

Zhang W, Purchio AF, Coffee R, West DB. Differential regulation of the human CYP3A4 promoter in transgenic mice and rats. Drug Metab Dispos 2004;32:163–167. [PubMed: 14744936]

Zhou Q, Yao TW, Yu YN, Zeng S. Stereoselective metabolism of propafenone by human liver CYP3A4 expressed in transgenic Chinese hamster CHL cells lines. Acta Pharmacol Sin 2001;22:944–948. [PubMed: 11749780]

NIH-PA Author Manuscript
NIH-PA Author Manuscript
NIH-PA Author Manuscript



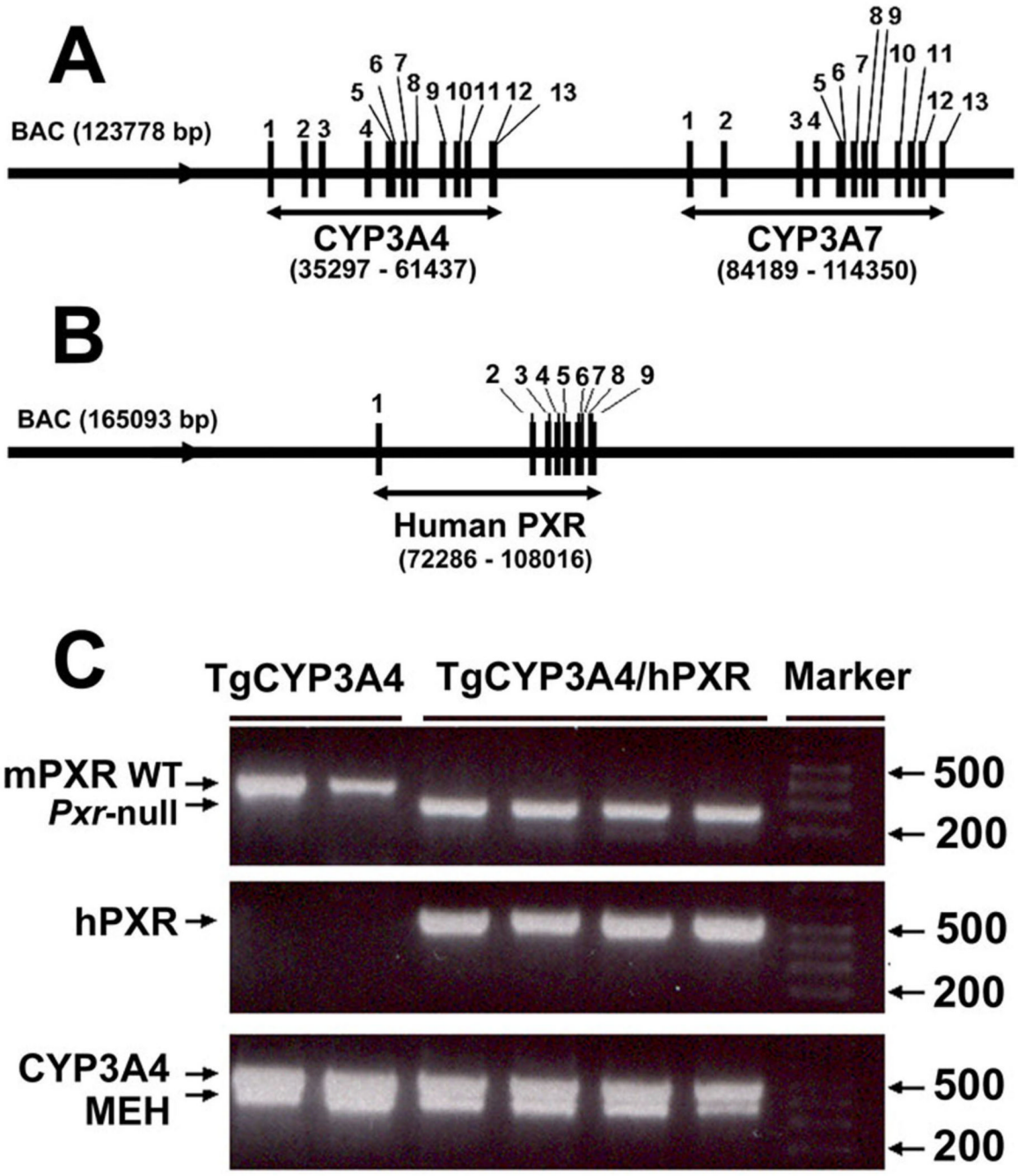


**Figure 1. Generation and genetic characterization of TgCYP3A4/hPXR mice**

(**A**) Structure of the BAC clone containing the complete human *CYP3A4* and *3A7* (exons 1-13) genes and the 5′-and 3′-flanking sequences. (**B**) Structure of the BAC clone containing the complete human *PXR* (exons 1-9) gene and the 5′- and 3′-flanking sequences. (**C**) A representative genotyping result for TgCYP3A4/hPXR mice. Mouse epoxide hydrolase 1 gene (MEH) primers served as an internal positive control. TgCYP3A4 mice were positive for the human *CYP3A4* transgene and containing the mouse *Pxr* allele. TgCYP3A4/hPXR mice were positive for both the human *PXR* and *CYP3A4* transgenes and containing the mouse *Pxr* null allele.

NIH-PA Author Manuscript
NIH-PA Author Manuscript
NIH-PA Author Manuscript



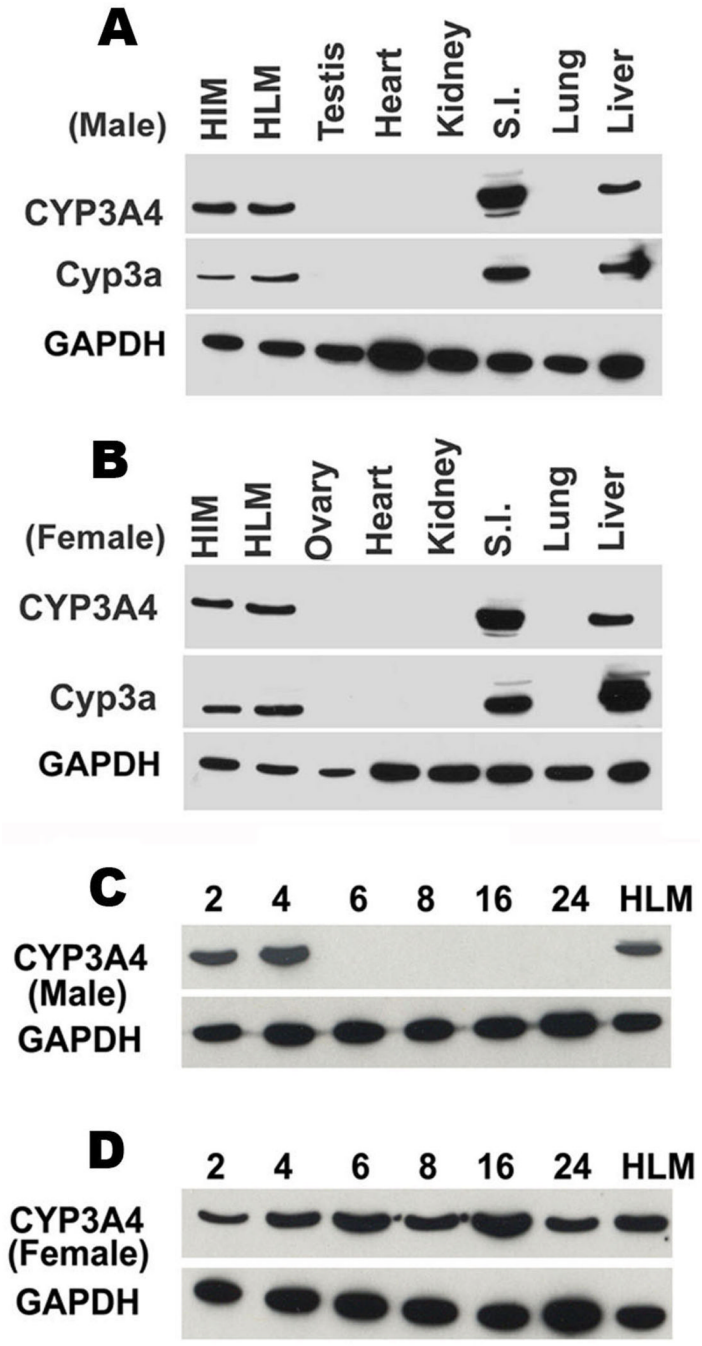


**Figure 2. Tissue distribution and developmental expression patterns of CYP3A4 in TgCYP3A4/hPXR mice**

(**A**, **B**) Liver, lung, small intestine (S.I.), kidney, heat, testis/ovary were collected from transgenic male (**A**) and female (**B**) mouse at 4-week-old; (**C**, **D**) Liver tissues were collected from transgenic male (**C**) and female (**D**) mice of different ages (2-24 weeks). All microsomes were prepared by differential centrifugation. Pooled microsomal samples (3-4 in each group) were used for western blot analysis. The monoclonal antibody against CYP3A4 (mAb 275-1-2) recognizes human CYP3A4 but not mouse Cyp3a or other liver proteins. The monoclonal antibody against Cyp3a (mAb 2-13-1) reacts with both mouse Cyp3a and human CYP3A4.

NIH-PA Author Manuscript

NIH-PA Author Manuscript

NIH-PA Author Manuscript

Human intestine microsomes (HIM) and human liver microsomes (HLM) served as positive controls for CYP3A4. GAPDH was used as loading control.

NIH-PA Author Manuscript

NIH-PA Author Manuscript

NIH-PA Author Manuscript

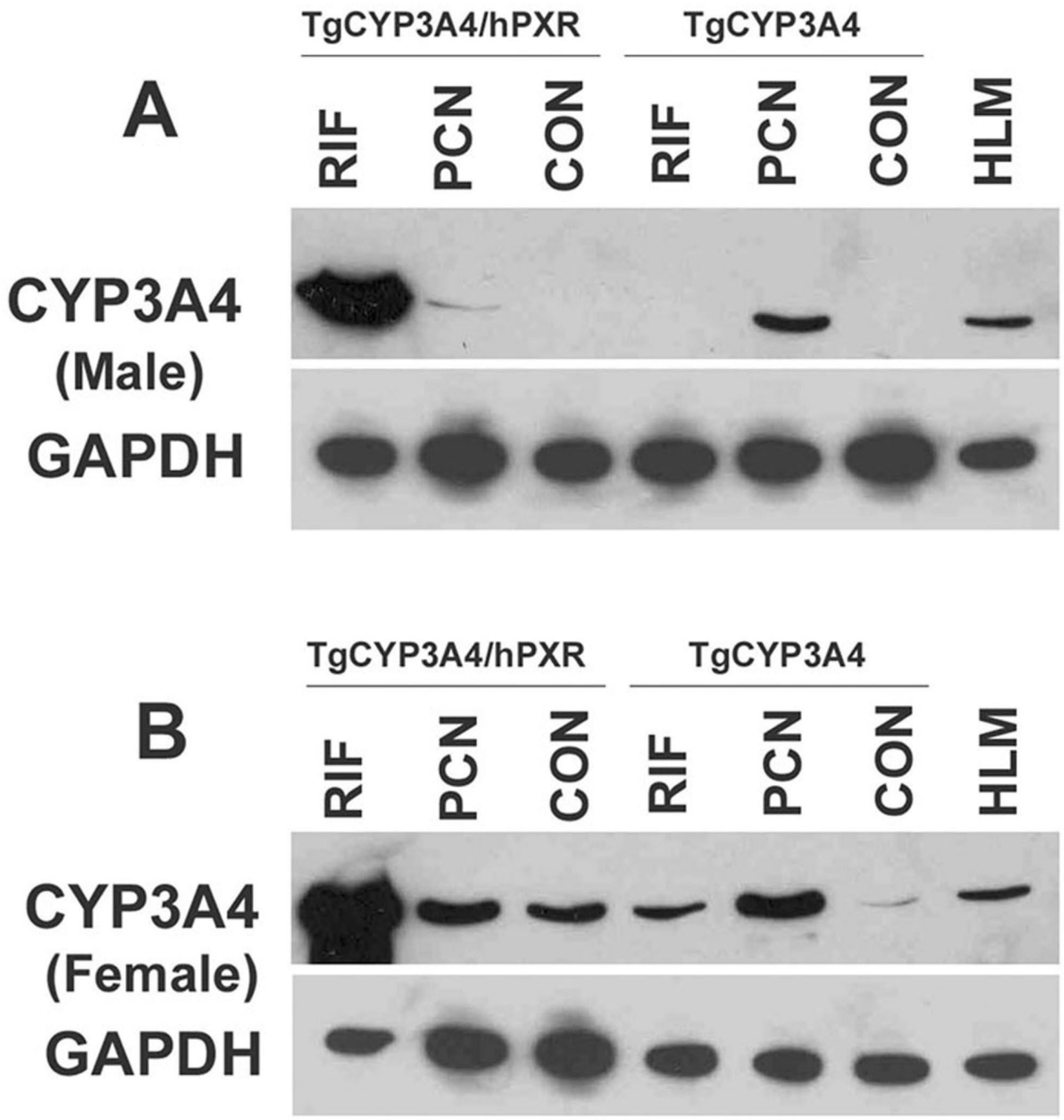


**Figure 3. Regulation of hepatic CYP3A4 in TgCYP3A4/hPXR mice**

TgCYP3A4 and TgCYP3A4/hPXR mice (8-week-old) were treated for three days with corn oil, 10 mg/kg/day PCN (ip), or 10 mg/kg/day RIF (po) as detailed under *Materials and Methods*. Liver was collected from transgenic male (**A**) and female (**B**) mice 24 h after the last dose. Pooled liver microsomes (3 samples) were prepared and analyzed by western blot. The monoclonal antibody against CYP3A4 (mAb 275-1-2) recognizes human CYP3A4 but not mouse Cyp3a or other liver proteins. Human liver microsome (HLM) served as positive control for CYP3A4. GAPDH was used as loading control.

NIH-PA Author Manuscript
NIH-PA Author Manuscript
NIH-PA Author Manuscript



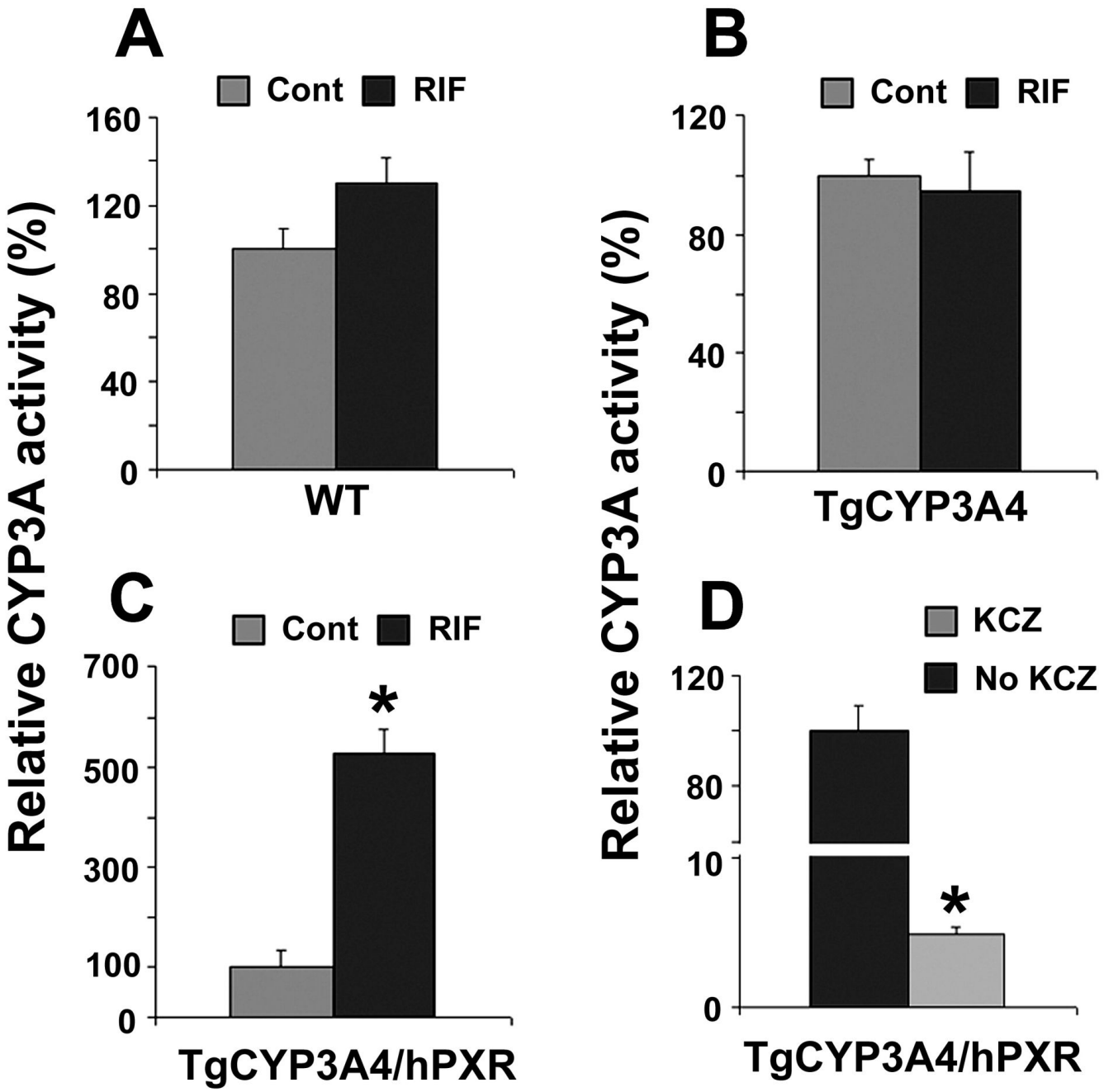


**Figure 4. CYP3A activity in liver microsomes of TgCYP3A4/hPXR mice**

All mice (male, 8-week-old) were treated with corn oil or 10 mg/kg/day RIF (po) for three days. Livers were collected 24 h after the last dose and microsomes were prepared. MDZ 1′-hydroxylation was used as the probe for CYP3A activity and detected by LC-MS/MS. CYP3A activity in each control group (Cont) was set as 100%. Data are expressed as means ± S.D., n=3. (**A**) CYP3A activity in WT mice. (**B**) CYP3A activity in TgCYP3A4 mice. (**C**) CYP3A activity in TgCYP3A4/hPXR mice and inhibition by ketoconazole (KCZ) (**D**). *$p < 0.05$ compared with no KCZ group.

NIH-PA Author Manuscript

NIH-PA Author Manuscript

NIH-PA Author Manuscript

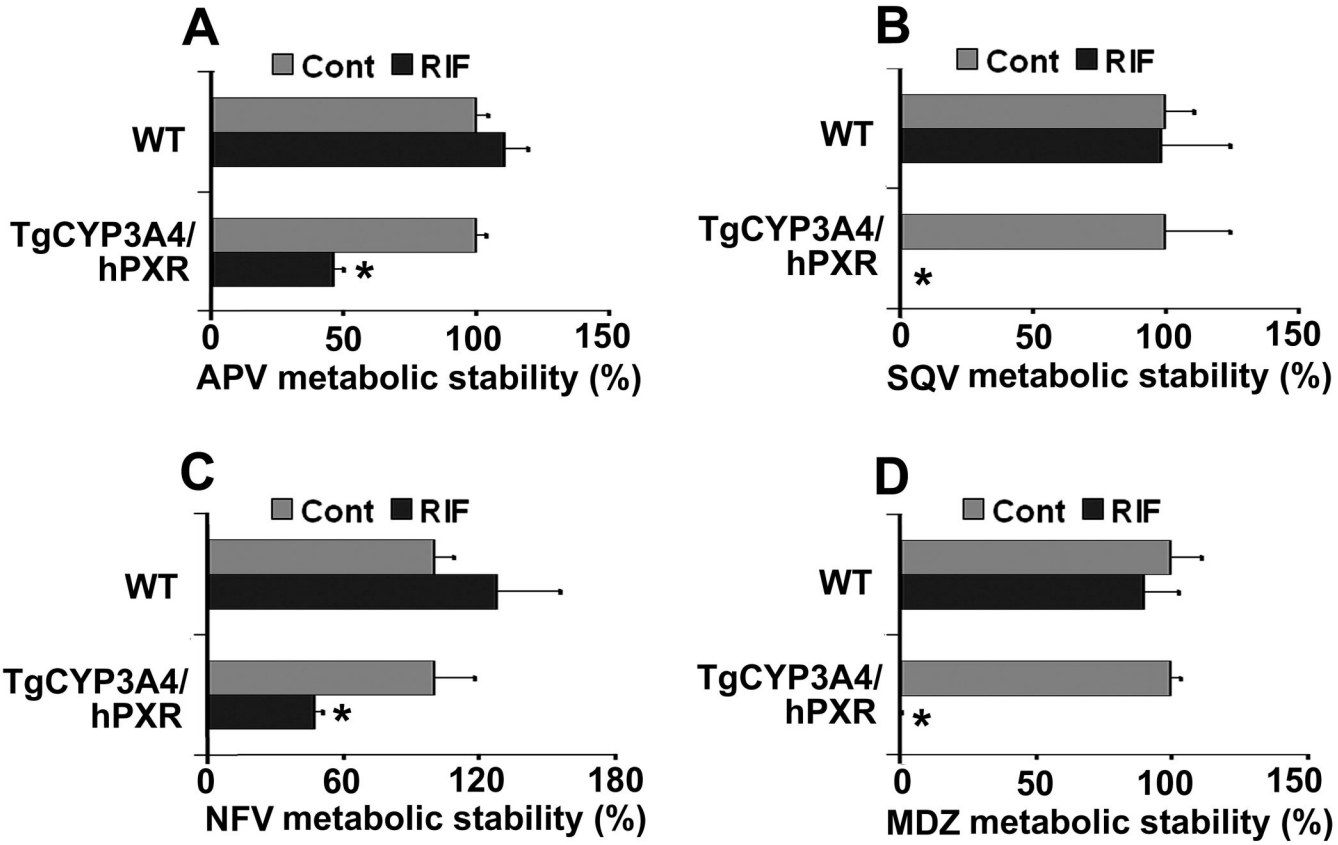


**Figure 5. PIs metabolic stability in liver microsomes of TgCYP3A4/hPXR mice**

All mice (male, 8-week-old) were treated with corn oil or 10 mg/kg/day RIF (po) for three days. Livers were collected 24 h after the last dose and microsomes were prepared. PIs metabolic stability was determined according to their metabolic rates by monitoring parent drug disappearance. APV, NFV, SQV and MDZ were detected by LC-MS/MS. Metabolic stability of APV (**A**), SQV (**B**), and NFV (**C**) was expressed as % of control (n=3). The metabolic stability in the control group was set at 100% for each chemical and each mouse line. Metabolic stability of MDZ (**D**) was used as positive control for these experiments. *$p <$ 0.05 compared with the corresponding control.

NIH-PA Author Manuscript
NIH-PA Author Manuscript
NIH-PA Author Manuscript



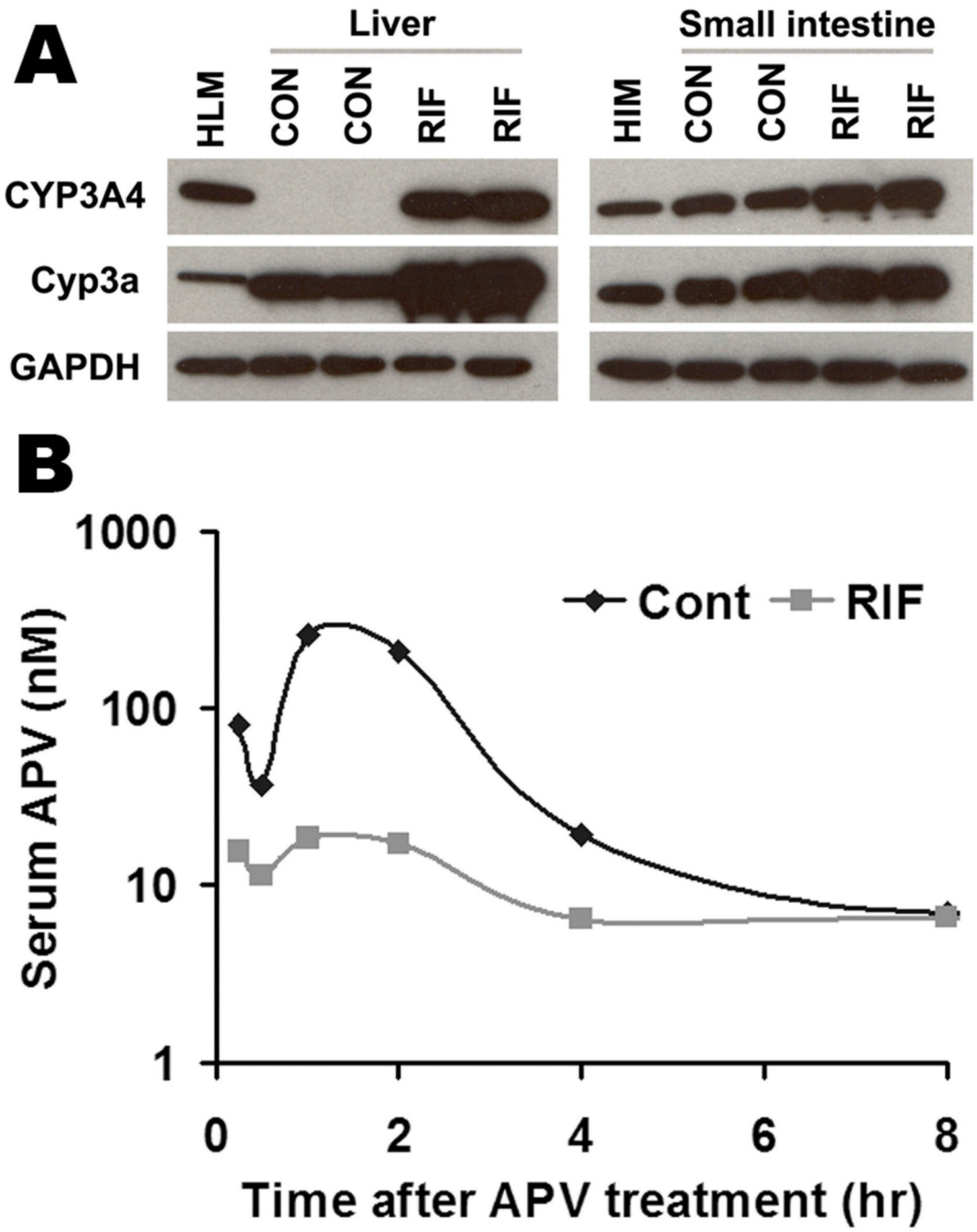


**Figure 6. Effect of RIF on APV metabolism *in vivo***

TgCYP3A4/hPXR mice were treated with purified diet (control) or modified diet with 100 mg/kg RIF for 6 days. On the 7$^{th}$ day, TgCYP3A4/hPXR mice were administered 50 mg/kg APV orally by gavage, and blood samples were collected at 0.25, 0.5, 1, 2, 4, 8, 18 hours after the treatment. (**A**) Expression of hepatic and intestinal CYP3A in TgCYP3A4/hPXR mice after 6 days treatment with RIF diet. Liver and intestine microsomes were prepared and analyzed by western blot. The monoclonal antibody against CYP3A4 (mAb 275-1-2) recognizes human CYP3A4 but not mouse Cyp3a or other liver proteins. The monoclonal antibody against Cyp3a (mAb 2-13-1) reacts with both mouse Cyp3a and human CYP3A4. Human liver microsome (HLM) and human intestine microsomes (HIM) served as positive control for CYP3A4.

GAPDH was used as loading control. (**B**) Time course of serum APV concentration (nM) was expressed as means (pooled sample, $n = 3$). APV was detected by LC-MS/MS.

NIH-PA Author Manuscript
NIH-PA Author Manuscript
NIH-PA Author Manuscript